

# Conformation, Dynamics, and Insertion of a Noncysteine-Containing Protegrin-1 Analogue in Lipid Membranes from Solid-State NMR Spectroscopy

Rajeswari Mani,<sup>[a]</sup> Alan J. Waring,<sup>[b]</sup> and Mei Hong<sup>\*[a]</sup>

Disulfide-bonded  $\beta$ -hairpin structures are common among antimicrobial peptides. Disulfide bonds are known to be important for antimicrobial activity, but the underlying structural reason is not well understood. We have investigated the membrane-bound structure of a disulfide-deleted analogue of the antimicrobial peptide protegrin-1, in which the four Cys residues were replaced by Ala. The secondary structure, dynamics, and topology of this Ala-PG1 peptide in the membrane were determined by using magic-angle-spinning NMR spectroscopy. Conformation-dependent  $^{13}\text{C}$  isotropic chemical shifts of multiple  $^{13}\text{C}$ -labeled residues were obtained from 1D cross-polarization and direct-polarization spectra, and from 2D J-coupling-mediated  $^{13}\text{C}$ - $^{13}\text{C}$  correlation spectra. Most labeled residues exhibited two conformations: a random coil and a  $\beta$ -sheet structure. The dual-conformation property was present in both anionic lipid bilayers, which mimic the bacterial membrane, and zwitterionic cholesterol-containing

bilayers, which mimic the eukaryotic cell membrane. The mobility of the peptide was measured by using a 2D C-H dipolar-shift correlation experiment. The random-coil fraction was highly mobile whereas the  $\beta$ -sheet component was rigid.  $^1\text{H}$  spin diffusion from the lipid chains to the peptide indicates that the  $\beta$ -sheet component was well inserted into the anionic membrane, but surface bound in the cholesterol-containing neutral membrane. Thus, the removal of disulfide bonds changed some PG-1 molecules to highly mobile random coils that were poorly associated with the lipid membrane, but other molecules retained a  $\beta$ -sheet conformation and had a similar membrane-binding topology to the parent peptide. Thus, the reduced antimicrobial activity of Ala-PG1 was largely due to the reduced number of insertion-competent  $\beta$ -sheet molecules, rather than uniformly weakened activity of identically structured peptides.

## Introduction

Antimicrobial peptides (AMPs) form part of the innate immune system of animals and plants and are involved in killing a broad range of pathogens by destroying their cell membranes.<sup>[1]</sup> They are capable of destroying microbes within minutes of contact, and are thus promising resistance-free antibiotics. Many structural-activity studies have been carried out to develop more potent antimicrobial sequences that have little or no cytotoxicity against host cells.<sup>[2]</sup>


Protegrin-1 (PG-1) is one of the first discovered disulfide-stabilized AMPs. It was isolated from porcine leukocytes<sup>[3]</sup> and is active against Gram-negative bacteria, Gram-positive bacteria, fungi, and viruses in the low  $\mu\text{g mL}^{-1}$  range.<sup>[4]</sup> A large number of mutations have been carried out on PG-1 to understand the structure-activity relationship.<sup>[2,5-7]</sup> A key finding has been that the two disulfide bonds in PG-1 are crucial for high antimicrobial activity and for maintaining the  $\beta$ -hairpin fold of the peptide. Substitution of all four cysteines in the wild-type peptide with alanine (Ala-PG1) results in markedly reduced activity:<sup>[2,5]</sup> the minimum inhibitory concentrations are more than 16-fold weaker than the wild-type peptide against methicillin-resistant *Staphylococcus aureus* and > 64-fold weaker against *Pseudomonas aeruginosa*.<sup>[2]</sup> On the other hand, when cysteines are mutated to threonines, which have high preference for a  $\beta$ -strand

conformation, and the original  $\beta$ -turn position of the parent peptide incorporates a turn-promoting  $\alpha$ -proline derivative, the  $\beta$ -hairpin fold is retained in solution and the peptide retains most of its antimicrobial potency.<sup>[6]</sup> Despite the rich information obtained from these structure-activity studies, little is known about the three-dimensional structure of PG-1 analogues in the lipid bilayer.

In this work, we use solid-state NMR spectroscopy to investigate the membrane-bound structure of the linear Cys-to-Ala PG-1 analogue, Ala-PG1. We have determined its conformation, dynamics, and depth of insertion in lipid bilayers of two different compositions, and compared them with those of wild-type

[a] R. Mani, Prof. M. Hong  
Department of Chemistry  
Iowa State University, Ames  
IA 50011 (USA)  
Fax: (+1) 515-294-0105  
E-mail: mhong@iastate.edu

[b] Prof. A. J. Waring  
Department of Medicine  
University of California at Los Angeles School of Medicine  
Los Angeles, California 90095 (USA)

 Supporting information for this article is available on the WWW under <http://www.chembiochem.org> or from the author.

PG-1, which has been extensively characterized by solid-state NMR spectroscopy.<sup>[8–13]</sup> Our previous study of Ala-PG1 with high-resolution  $^1\text{H}$  NMR spectroscopy showed that the peptide is completely unstructured in solution.<sup>[5,14]</sup> However, when bound to the lipid membrane, Ala-PG1 exhibits  $^{13}\text{C}$  isotropic chemical shifts that are indicative of both the random-coil conformation and  $\beta$ -strand structure. These  $^{13}\text{C}$  chemical shifts are obtained from a combination of 1D and 2D correlation spectra that selectively detect either rigid or mobile components, and the random-coil fraction is found to be highly dynamic. Quantitative C–H dipolar couplings were measured to confirm that the random-coil molecules undergo large-amplitude motion while the  $\beta$ -sheet component is nearly completely immobilized. Lipid-to-peptide  $^1\text{H}$  spin-diffusion experiments indicated that the  $\beta$ -sheet fraction of Ala-PG1 has a similar membrane-specific insertion motif as the wild-type peptide—it inserts into anionic POPE/POPG membranes but remains on the surface of zwitterionic POPC/cholesterol membranes. These results give insights into the origin of the reduced antimicrobial activity of the disulfide-deleted peptide.

## Results

### Backbone conformation of Ala-PG1 from $^{13}\text{C}$ chemical shifts

Figure 1 shows the  $^{13}\text{C}$  magic-angle-spinning (MAS) spectra of (Phe12, Ala13, Val14)-labeled Ala-PG1 in POPE/POPG (3:1) membranes at a peptide/lipid (P/L) molar ratio of 1:15. Each

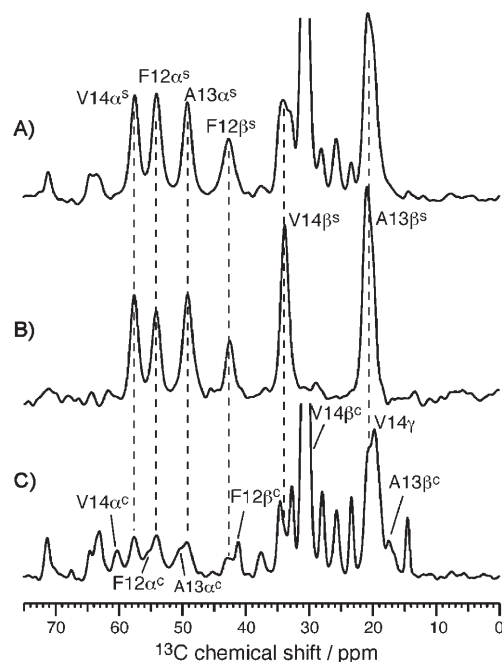


**Figure 1.** One dimensional  $^{13}\text{C}$  MAS spectra of (Phe12, Ala13, Val14)-labeled Ala-PG1 in POPE/POPG (3:1) membranes at 298 K. A) CP spectrum showing  $\beta$ -sheet signals (denoted by the superscript, s). B) Double-quantum-filtered CP spectrum removed the lipid peaks and selected only the peptide signals. C) DP spectrum showing additional signals from the random-coil fraction (denoted by the superscript, c). Dashed lines are used to guide the eye for peak assignment.

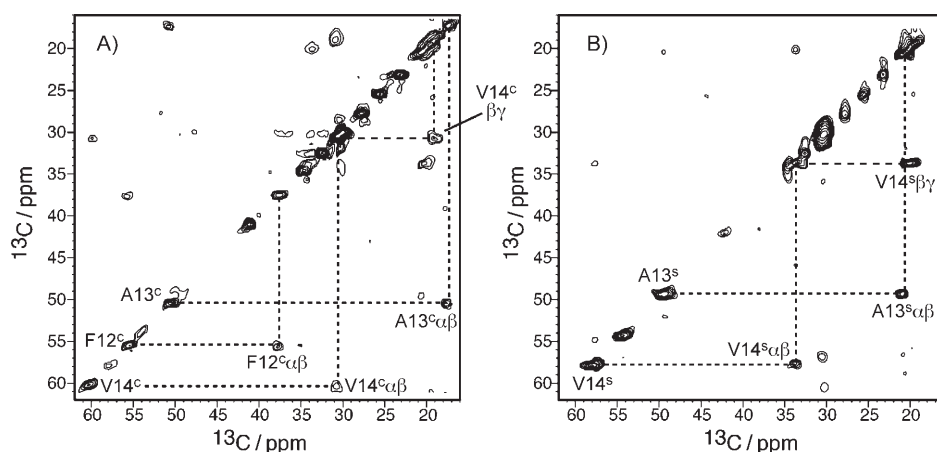
residue was uniformly labeled with  $^{13}\text{C}$  and  $^{15}\text{N}$ . The peaks were assigned based on the characteristic  $^{13}\text{C}$  chemical shifts of amino-acid residues in proteins.<sup>[15]</sup> The  $\text{C}\alpha$  and  $\text{C}\beta$  shifts of all three residues in the cross-polarization (CP) spectrum indicate  $\beta$ -sheet conformation (Figure 1A): the  $\text{C}\alpha$  chemical shifts are smaller than the random-coil values while the  $\text{C}\beta$  chemical shifts are larger than the random-coil values. To simplify the spectra and remove the background lipid  $^{13}\text{C}$  signals, we applied a double-quantum filter (DQF) in which SPC-5 was used as the  $^{13}\text{C}$ – $^{13}\text{C}$  mixing sequence.<sup>[16]</sup> The DQF removed the lipid-chain signals that overlapped with Val  $\text{C}\beta$  and Ala  $\text{C}\beta$ , and thus clarified the peak assignment (Figure 1B).

It is well known that  $^1\text{H}$ ,  $^{13}\text{C}$  cross-polarization selectively detects rigid components in a mixture due to its requirement for  $^1\text{H}$ – $^{13}\text{C}$  dipolar couplings. The signals of mobile segments are suppressed because motion reduces the dipolar coupling. To observe all possible conformational and dynamical components in Ala-PG1, we measured a direct polarization (DP)  $^{13}\text{C}$  spectrum, in which a  $^{13}\text{C}$   $90^\circ$  pulse was used to excite the  $^{13}\text{C}$  magnetization. The DP experiment preferentially detects mobile components because it does not require dipolar couplings and because mobile segments have short  $^{13}\text{C}$   $T_1$  relaxation times. Indeed, the DP spectrum of Ala-PG1 shows a more complex pattern with two peaks for each  $\text{C}\alpha$  and  $\text{C}\beta$  label (Figure 1C). In addition to the  $\beta$ -sheet signals, the second set of signals had chemical-shift characteristics of a random-coil conformation. Its presence in the DP but not the CP spectrum indicates that this random-coil fraction is mobile, as expected for this conformation.

To further enhance the spectral resolution and better distinguish the coil and sheet resonances, we carried out a 2D-correlation experiment, CTUC–COSY<sup>[17]</sup> to assign the  $^{13}\text{C}$  resonances. This experiment utilizes  $^{13}\text{C}$ – $^{13}\text{C}$   $J$  coupling to transfer the  $^{13}\text{C}$  coherence,<sup>[17,18]</sup> which is necessary for observing cross peaks of mobile molecules. We combined the CTUC–COSY sequence with DP to detect the mobile portion of Ala-PG1 and with CP to detect the rigid component of the peptide. The experiments were carried out at 298 K, in the liquid-crystalline (LC) phase of POPE/POPG bilayers. Only labeled peptide  $^{13}\text{C}$  sites can give cross peaks, while the background lipid  $^{13}\text{C}$  signals are observed along the diagonal.

Figure 2 shows the 2D CTUC–COSY spectra of (Phe12, Ala13, Val14)-labeled Ala-PG1 in POPE/POPG membranes with DP (Figure 2A) and CP (Figure 2B) as the magnetization-excitation method. A total  $J$  coupling mixing time of 10.8 ms was used. Clear  $\text{Ala}\alpha\beta$ ,  $\text{Phe}\alpha\beta$ ,  $\text{Val}\alpha\beta$ , and  $\text{Val}\beta\gamma$  cross peaks were observed for both the random coil and  $\beta$ -sheet fractions of the peptide. From these spectra we obtained accurate chemical shifts for  $\text{C}\alpha$  and  $\text{C}\beta$ , which are sensitive to the backbone conformation.

The same 1D CP and DP experiments and 2D CTUC–COSY experiments were applied to (Leu5, Ala6, Phe7)-labeled Ala-PG1 and (Ala15, Val16)-labeled Ala-PG1. The resulting spectra confirmed the presence of both random-coil and  $\beta$ -sheet conformations in these regions of the peptide (Figures S1 and S2 in the Supporting Information). Table 1 summarizes the  $\text{C}\alpha$  and  $\text{C}\beta$  chemical shifts of all labeled sites of Ala-PG1 in the POPE/



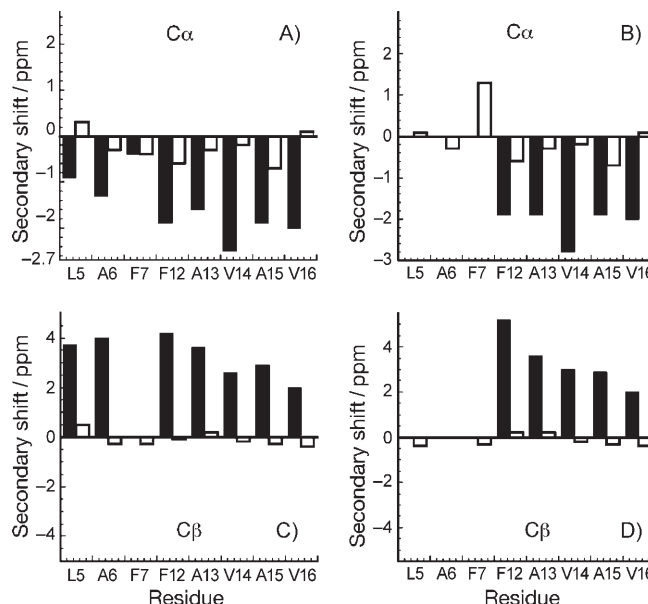
**Figure 2.** Two dimensional  $^{13}\text{C}$ - $^{13}\text{C}$   $J$ -coupling mediated CTUC-COSY spectra of (Phe12, Ala13, Val14)-Ala-PG1 in POPE/POPG membranes. A) The  $^{13}\text{C}$  magnetization was prepared by using DP. B) The  $^{13}\text{C}$  magnetization was prepared by using CP. Superscripts c and s denote random coil and  $\beta$ -sheet signals, respectively. The total  $J$ -mixing time was 10.8 ms; spectra were acquired at 298 K under 9 kHz MAS.

Table 1. $^{13}\text{C}$ $\text{C}\alpha$ and $\text{C}\beta$ chemical shifts (ppm) of labeled residues in Ala-PG1 in POPE/POPG membranes.			
Residue	Sites	$\delta$ coil	$\delta$ sheet
Leu5	$\text{C}\alpha$	53.5	52.3
	$\text{C}\beta$	41.2	44.4
Ala6	$\text{C}\alpha$	50.8	49.8
	$\text{C}\beta$	17.1	21.4
Phe7	$\text{C}\alpha$	55.9	-
	$\text{C}\beta$	37.5	-
Phe12	$\text{C}\alpha$	55.7	54.4
	$\text{C}\beta$	37.7	42.0
Ala13	$\text{C}\alpha$	50.8	49.5
	$\text{C}\beta$	17.6	21.0
Val14	$\text{C}\alpha$	60.2	57.9
	$\text{C}\beta$	30.8	33.6
Ala15	$\text{C}\alpha$	50.4	49.2
	$\text{C}\beta$	17.1	20.3
Val16	$\text{C}\alpha$	60.5	58.4
	$\text{C}\beta$	30.6	33.0

POPG membrane. Phe7 did not exhibit any  $\beta$ -sheet signal in the CP spectrum; this suggests that there is intermediate timescale motion at this residue in the  $\beta$ -sheet peptide, which interferes with cross polarization and  $^1\text{H}$  dipolar decoupling.

To determine if Ala-PG1 conformation is affected by membrane composition, we repeated the chemical-shift measurements in POPC/cholesterol membranes. Most chemical shifts were similar to those measured in the POPE/POPG membrane, except that Leu5, Ala6, and Phe7 only exhibited random-coil and no  $\beta$ -sheet signals. Thus, the intermediate timescale motion of Phe7 implied in the POPE/POPG membrane appears to be present in the POPC/cholesterol membrane as well, and affects more residues than in the POPE/POPG membrane.

Figure 3 summarizes the  $\text{C}\alpha$  and  $\text{C}\beta$  secondary shifts of all labeled residues, and was obtained by subtracting the observed chemical shifts by the random-coil shifts.<sup>[19]</sup> The rigid component ( $\blacksquare$ ) exhibited large negative  $\text{C}\alpha$  secondary shifts and positive  $\text{C}\beta$  secondary shifts; this indicates a  $\beta$ -sheet conformation.



**Figure 3.** The  $^{13}\text{C}$  secondary shifts of Ala-PG1 in: A) and C) POPE/POPG (3:1) membranes, and B) and D) POPC/cholesterol (1.2:1) membranes. Filled bars indicate the rigid component of the peptide detected in the CP spectra, and open bars denote the mobile component observed in the DP spectra. Negative  $\text{C}\alpha$  secondary shifts and positive  $\text{C}\beta$  secondary shifts indicate the  $\beta$ -sheet conformation.

excite the  $^{13}\text{C}$  magnetization. Figure 4 shows several representative doubled-DIPSHIFT curves for Ala-PG1 in POPE/POPG membranes. The true  $\text{C}\alpha$ - $\text{H}\alpha$  dipolar couplings, which were obtained by dividing the observed couplings by the MREV-8 scaling factor of 0.47 and the doubling factor of 2, ranged from 2.5 to 6.8 kHz for the coil conformation but were close to the rigid limit of 22.7 kHz for the  $\beta$ -sheet conformation. The  $\text{C}\alpha$ - $\text{H}\alpha$  order parameters were obtained by dividing these true couplings by the rigid-limit value of 22.7 kHz (Table 2). Some dipolar dephasing data did not completely fit with a single coupling, but required a small range of dipolar couplings. We

The mobile component ( $\square$ ) exhibited small secondary shifts; this indicates a random-coil conformation.

### Dynamics of Ala-PG1 in anionic and neutral lipid membranes

To probe the dynamics of Ala-PG1 in lipid bilayers we carried out a C-H doubled-DIPSHIFT experiment,<sup>[20]</sup> which measures C-H dipolar coupling in the  $\omega_1$  dimension as resolved by  $^{13}\text{C}$  chemical shifts. To capture both the mobile and rigid components, DP and CP were used to

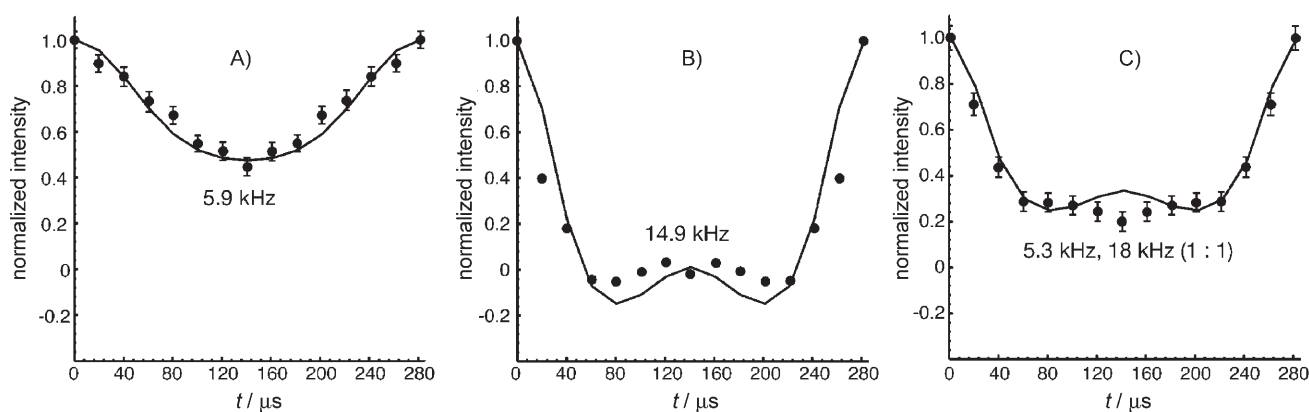


**Figure 4.** Representative C–H dipolar dephasing curves of Ala-PG1 in POPE/POPG membranes, extracted from the indirect dimension of 2D DIPSHIFT spectra. A) The Val14 C $\alpha$  cross section at 60.3 ppm corresponds to the random-coil conformation. A DP–DIPSHIFT experiment was used to obtain the data. B) The Val14 C $\alpha$  cross section at 57.6 ppm corresponds to the  $\beta$ -sheet conformation. A CP–DIPSHIFT experiment was used to obtain the data. C) The Phe12 C $\alpha$  cross section at 55.7 ppm was obtained from a DP–DIPSHIFT experiment. The best-fit true dipolar couplings, which were obtained by dividing the observed couplings by the MREV-8 scaling factor and the doubling factor, are indicated for each dephasing curve.

**Table 2.** C $\alpha$ –H $\alpha$  dipolar order parameters,  $S_{\text{CH}}$ , for labeled residues in Ala-PG-1 in POPE/POPG and POPC/cholesterol membranes.

Residue	POPE/POPG		POPC/cholesterol	
	$S_{\text{CH}}$ coil	$S_{\text{CH}}$ sheet	$S_{\text{CH}}$ coil	$S_{\text{CH}}$ sheet
Leu5	0.14–0.23	0.80–0.90	0.19	–
Ala6	0.19–0.23	0.80–0.90	0.23	–
Phe7	0.26–0.30	–	0.19–0.21	–
Phe12	0.19–0.30	0.80	–	1.0
Ala13	0.19–0.23	1.0	0.33–0.39	1.0
Val14	0.26	0.56–0.66	0.19	0.98
Ala15	0.12	1.0	0.21	1.0
Val16	0.11–0.14	0.94–0.98	0.12–0.14	0.75–0.80

express these results as an order parameter range. For residues for which the coil-sheet isotropic peaks were not well resolved, the dephasing data were found to be best fit by using a mixture of small and large dipolar couplings. An example is shown for Phe12 (Figure 4C) for which the dephasing curve was best fit by using a 1:1 mixture of 5.3 and 18 kHz, which represent the couplings for the coil and sheet fractions, respectively.

Table 2 quantitatively shows that in the POPE/POPG membrane Ala-PG1 had low-order parameters of 0.11 to 0.30 for the random-coil component, but had larger-order parameters of 0.80 or higher for most sites of the  $\beta$ -sheet component. This indicates that the random-coil peptide backbone undergoes large-amplitude motions while the  $\beta$ -sheet conformation is mostly rigid. The same difference was observed in the POPC/cholesterol membrane; this indicates that peptide mobility was little affected by membrane composition.

#### Location of Ala-PG1 in anionic and neutral lipid bilayers

Since the random-coil fraction of Ala-PG1 was highly mobile, it was most likely only loosely, if at all, associated with the membrane, and thus retained its solution-state conformation.<sup>[14]</sup> But whether the rigid  $\beta$ -sheet fraction inserts into the anionic lipid membrane like the parent peptide is not clear. To determine

the depth of insertion of the  $\beta$ -sheet fraction, we carried out lipid-to-protein  $^1\text{H}$  spin-diffusion experiments. The experiment detects  $^1\text{H}$  spin diffusion from mobile lipids to the rigid peptide by correlating the lipid  $^1\text{H}$  signals with peptide  $^{13}\text{C}$  signals. The experiment requires  $^1\text{H}$ – $^{13}\text{C}$  cross polarization and immobilized peptide, thus the mobile fraction of Ala-PG1 was not detected. Figure 5A shows a representative 2D spectrum of (Phe12, Ala13, Val14)-labeled Ala-PG1 in POPE/POPG bilayers, and was measured with a spin diffusion mixing time of 529 ms. The cross-peak intensity between the peptide  $^{13}\text{C}$  and lipid  $\text{CH}_2$  and water protons indicates the proximity of the peptide to the middle and surface of the lipid bilayer, respectively. Figure 5B shows the sum of the  $^1\text{H}$  cross sections at the three C $\alpha$  slices and the Phe12 C $\beta$  slice. The  $\text{CH}_2$  peak was already visible at a short mixing time of 100 ms; this indicates that the peptide lies near the lipid acyl chains.

To quantify the minimal distance between the peptide and the lipid  $\text{CH}_2$  or  $\text{H}_2\text{O}$  groups, we plotted the cross-peak intensities as a function of the square root of the mixing time.<sup>[21]</sup> The intensities were corrected for  $^1\text{H}$   $T_1$  relaxation and normalized to the 100 ms  $\text{H}_2\text{O}$  peak intensity (Figure 5C). Further, since the equilibrium  $\text{CH}_2$  intensity was only 62% of the  $\text{H}_2\text{O}$  intensity, as seen in the 1D  $^1\text{H}$  direct-excitation spectrum, the  $\text{CH}_2$  cross-peak intensities from the 2D spectra were divided by 0.62 to reflect the fact that even after complete equilibration of the  $^1\text{H}$  magnetization, the  $\text{CH}_2$  intensity will still only be 62% of the  $\text{H}_2\text{O}$  intensity. The resulting experimental buildup curve was fit by using a 1D lattice model for magnetization transfer.<sup>[21]</sup> The diffusion coefficients for the lipid and peptide were 0.012 and 0.3  $\text{nm}^2\text{ms}^{-1}$ , respectively, which were similar to the values used and estimated previously.<sup>[21,22]</sup> For the lipid–peptide interface, a diffusion coefficient of 0.0005  $\text{nm}^2\text{ms}^{-1}$  was found to best reproduce the shape of the buildup curve. The resulting gap between the peptide and lipid chain  $\text{CH}_2$  groups was found to be 6 Å. This was 4 Å longer than the wild-type peptide, and indicates that Ala-PG1 inserts into the lipid-chain region but does not fully reach the center of the membrane. The  $\text{H}_2\text{O}$  buildup curve, which was simulated by

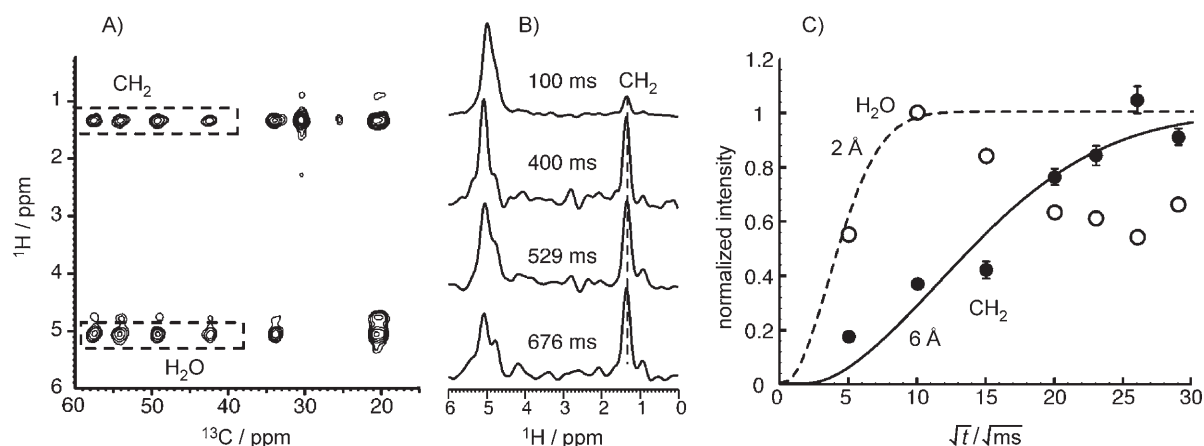


**Figure 5.**  $^1\text{H}$  spin diffusion data of Ala-PG1 in POPE/POPG membranes. A) 2D  $^{13}\text{C}$ -detected  $^1\text{H}$  spin diffusion spectrum of (Phe12, Ala13, Val14)-labeled Ala-PG1 at a mixing time of 529 ms. Only the rigid component of the peptide was detected; dashed lines indicate the  $^{13}\text{C}$  slices summed for display in B). B) Sum of the  $^1\text{H}$  cross sections of peptide  $^{13}\text{C}$  signals at various mixing times. C)  $\text{CH}_2$  (●) and  $\text{H}_2\text{O}$  (○) buildup curves after  $^1\text{H}$   $T_1$  correction, normalization to the water peak at 100 ms, and normalization to the equilibrium intensity. Best-fit curves for  $\text{CH}_2$  (—) and  $\text{H}_2\text{O}$  (----) were obtained with a distance of 6 and 2 Å, respectively.

using diffusion coefficients of  $0.03 \text{ nm}^2 \text{ ms}^{-1}$  for water and  $0.00225 \text{ nm}^2 \text{ ms}^{-1}$  for the peptide–water interface, rose faster than the  $\text{CH}_2$  buildup curve; this indicates that some of the residues in the Ala-PG1  $\beta$ -sheet were exposed to water.

In the POPC/cholesterol membrane, the  $\text{CH}_2$ -to-peptide  $^1\text{H}$  spin-diffusion buildup curve rose much more slowly than in the POPE/POPG bilayers. A representative 2D spectrum and the sum of the  $\text{C}\alpha$   $^1\text{H}$  cross sections are shown in Figure 6A and B. The  $\text{CH}_2$  peak was not visible until 400 ms. Buildup curves for the  $\text{CH}_2$  and  $\text{H}_2\text{O}$  peaks are shown in Figure 6C. The  $\text{H}_2\text{O}$  buildup curve was fit by using a distance of 4.0 Å, but the  $\text{CH}_2$  buildup was much slower and was best fit with a distance of 25 Å. Thus, Ala-PG1 lies on the surface of the POPC/cholesterol membrane, far from the hydrophobic core of the bilayer.

## Discussion

The above data indicate that the Cys-to-Ala analogue of PG-1 exhibits a mixture of random-coil and  $\beta$ -sheet conformations that have different dynamics and insertion depths in the lipid membrane. This differs from the conformation of Ala-PG1 in aqueous solution, which is completely unstructured, as shown by  $^1\text{H}$  high-resolution NMR spectra.<sup>[14]</sup> Thus, the lipid bilayer promotes partial folding of the peptide to the  $\beta$ -sheet conformation. This suggests that apart from the disulfide bonds, the amino-acid sequence of PG-1 encodes a preference for the  $\beta$ -sheet conformation. This coil-to-sheet conformational change as the peptide binds to the membrane is observed for both POPE/POPG and POPC/cholesterol bilayers. Previous CD experi-

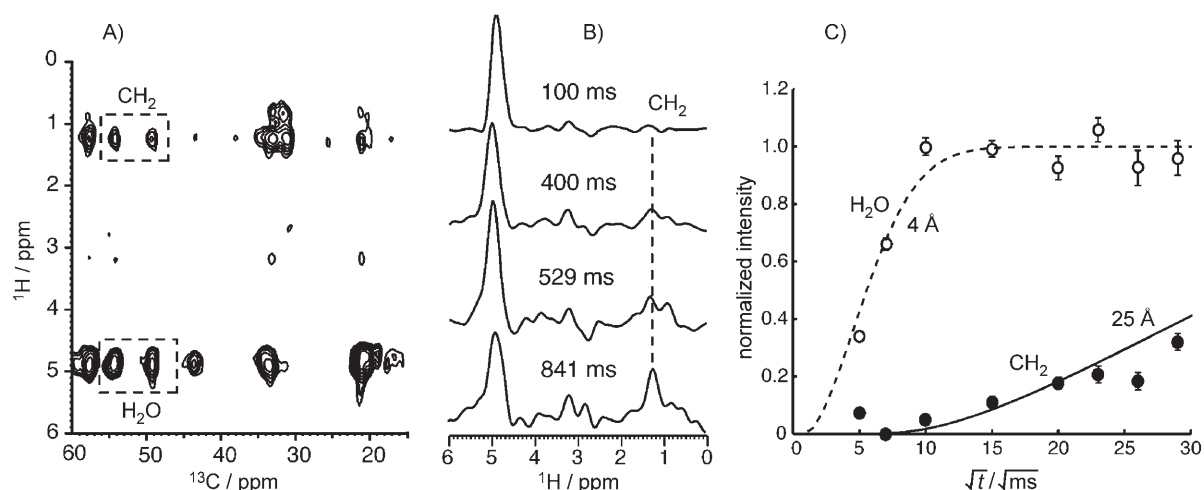


**Figure 6.**  $^1\text{H}$  spin-diffusion data of Ala-PG1 in POPC/cholesterol membranes. A) 2D  $^{13}\text{C}$ -detected  $^1\text{H}$  spin-diffusion spectrum of (Phe12, Ala13, Val14)-labeled Ala-PG1 at a mixing time of 841 ms. Only the rigid component of the peptide was detected. B) Sum of the  $^1\text{H}$  cross sections of Phe12 and Ala13  $\text{C}\alpha$  for various mixing times. The  $\text{CH}_2$  signal was absent until 400 ms. C)  $\text{CH}_2$  (●) and  $\text{H}_2\text{O}$  (○) buildup curves. Best-fit curves for  $\text{CH}_2$  (—) and  $\text{H}_2\text{O}$  (----) were obtained with a distance of 25 and 4 Å, respectively.

ments on Ala-PG1 bound to simulated *S. aureus* and *E. coli* lipids indicated a combination of  $\alpha$ -helical and  $\beta$ -sheet conformations for P/L higher than 1:30, and increased helical content at lower P/L.<sup>[5]</sup> These data suggest that the  $\beta$ -sheet conformation of Ala-PG1 is enhanced by high peptide concentrations; this is consistent with the strong  $\beta$ -sheet signals seen in the P/L (1:15) spectra here. The NMR spectra directly resolve the random-coil and  $\beta$ -sheet conformations through their distinct frequencies; thus the conformational heterogeneity is unambiguous. The lack of the  $\alpha$ -helical conformation in the NMR samples compared to the CD data could be partly due to the higher peptide concentration of the NMR samples. However, it should be noted that CD spectroscopy of membrane-bound proteins suffers from background scattering from lipid vesicles, thus is a less reliable method than NMR spectroscopy, in which lipid signals are usually well resolved from peptide signals and lipid signals can be further filtered out by double-quantum experiments.

The dynamical difference between the two conformations of Ala-PG1 as measured by the C–H dipolar couplings and the CP/DP spectral comparison confirms the expectation that the random-coil fraction is highly mobile whereas the  $\beta$ -strand fraction is immobilized. The latter data suggest that the  $\beta$ -strand Ala-PG1 inserts as oligomers in the membrane. Oligomerization reduces the exposure of polar backbone groups such as N–H and C=O to the hydrophobic lipid chains, and has been detected and characterized in detail in wild-type PG-1.<sup>[12,22]</sup>

An increasing number of proteins in the solid state have recently been observed to exhibit intramolecular dynamic heterogeneity, so that a part of the protein gives clear signals in the NMR spectra while other residues are invisible.<sup>[23,24]</sup> However, few proteins have been reported to exhibit dramatic dynamic heterogeneity between different molecules as a result of conformational differences. In the present case, this heterogeneity is clearly due to binding to the lipid membrane, since in the absence of the lipid bilayer the peptide was completely random coil. The ability of the lipid bilayer to induce  $\beta$ -strand formation from an unstructured peptide is a remarkable finding of this study.

The depth of insertion of the  $\beta$ -sheet Ala-PG1 differs between the anionic membrane and the zwitterionic cholesterol-containing membrane: the peptide inserts into the hydrophobic region of the anionic membrane but remains surface bound in the cholesterol-containing membrane. This membrane-specific topology is very similar to wild-type PG-1.<sup>[22]</sup> The only difference is that wild-type PG-1 inserts all the way to the center of the anionic membrane with a minimum distance of 2 Å to the CH<sub>2</sub> groups, while Ala-PG1 has a somewhat longer minimum distance of 6 Å. The inserted topology of the  $\beta$ -strand Ala-PG1 is distinct from the random-coil conformation of the peptide, which is either not associated or only loosely affiliated with the membrane.

The bimodal nature of Ala-PG1 structure and the similarity of the  $\beta$ -strand conformer to the wild-type peptide in terms of dynamics and insertion depths suggest that the reduced antimicrobial activity of Ala-PG1 is both due to the reduced

amount of the peptide able to bind to the lipid membrane to inflict damage, and to a possible weakening of the bound peptide's membrane-disruptive ability. Our previous <sup>31</sup>P NMR line-shape analysis of glass-plate oriented lipid membranes showed that Ala-PG1 causes less, but not zero, membrane disorder compared to wild-type PG-1.<sup>[14]</sup> As judged from the <sup>31</sup>P line-shape, the amount of disorder induced by Ala-PG1 is ~20-times lower than that of the wild-type PG-1,<sup>[14]</sup> this is in rough agreement with the 16–64-fold reduction in antimicrobial activity. Since the amount of the  $\beta$ -sheet intensity in the <sup>13</sup>C MAS spectra is clearly more than 10% but rather approximately half of the total intensity of each site, the random-coil fraction of the peptide should only reduce the antimicrobial activity by a factor of 2–3. The actual one order of magnitude reduction in activity implies that the inserted  $\beta$ -sheet fraction of the Ala-PG1 mutant is much less active than the wild-type peptide.

The current data do not indicate whether the  $\beta$ -strand fraction of Ala-PG1 folds into  $\beta$  hairpins or remains as  $\beta$  strands. The key potential sites for the  $\beta$  turn, Arg9, Arg10, and Arg11, were not labeled here due to the high cost of labeling with Arg. If the rigid fraction of Ala-PG1 exists as a straight strand, then its intrinsic membrane-lytic activity should be lower than the  $\beta$  turn parent molecule because of the lower amphiphilicity of the linear molecule. The importance of the  $\beta$ -hairpin fold for antimicrobial activity has been examined by solution NMR and circular dichroism studies,<sup>[6]</sup> and has been reported in a related peptide, tachyplesin.<sup>[25–27]</sup>

The present work points to the importance of using <sup>13</sup>C direct-polarization and *J*-coupling-based polarization transfer experiments to detect mobile components in membrane proteins by NMR. The <sup>13</sup>C DP CTUC–COSY experiment is ideal for this purpose. The cross peaks of the mobile components in the 2D CTUC–COSY spectra are well resolved by the use of constant-time evolution and by linear prediction, and the cross-peak intensities relative to the diagonal peaks are also higher than in dipolar-driven correlation experiments.

In summary, we have determined the membrane-bound conformation, dynamics, and topology of a linear analogue of protegrin-1, and found that the removal of the cysteine disulfide bonds results in a mixture of random-coil and  $\beta$ -sheet conformations. The former is highly dynamic and likely not associated with the lipid membrane, whereas the latter is rigid and inserts into the anionic lipid bilayer, similar to the parent peptide, PG-1. Thus, the reduced antimicrobial activity of the linear peptide is due to the reduced number of insertion-competent membrane-lytic  $\beta$ -sheet molecules, rather than uniformly weakened activity of identically structured peptides.

## Experimental Section

**Sample preparation:** All lipids were purchased from Avanti Polar Lipids (Alabaster, AL, USA) and used without further purification. Uniformly <sup>13</sup>C- and <sup>15</sup>N-labeled amino acids were purchased from Sigma–Aldrich and Cambridge Isotope Laboratories (Andover, MA, USA). The Ala-PG1 sequence differs from wild-type PG-1 in that all four Cys residues at positions 6, 8, 13, and 15 were replaced by Ala (NH<sub>2</sub>-RGGRLAYARRRFAVAVGR-CONH<sub>2</sub>). It was synthesized by using

standard Fmoc solid-phase peptide synthesis protocols, and purified to 95% by using reverse-phase HPLC. Three peptide samples, which incorporated labeled Leu5, Ala6, Phe7 (sample 1), Phe12, Ala13, Val14 (sample 2), and Ala15, Val16 (sample 3), were synthesized.

The peptides were reconstituted in lipid membranes by mixing lipids and peptide first in trifluoroethanol/methanol (3:1). The solvents were vacuum dried and the resulting peptide–lipid film was packed in a rotor and hydrated to 35% with water. All membrane samples had a peptide/lipid molar ratio (P/L) of 1:15. Only phospholipids, POPC, POPE, and POPG, but not cholesterol, were included in the lipid molar amount calculation. A POPE/POPG (3:1) mixture was used to mimic the bacterial cell membrane, and a POPC/cholesterol mixture (12:10.5) was used to mimic the red blood cell membrane.

**NMR spectroscopy:** Solid-state NMR spectroscopy experiments were carried out by using a Bruker DSX-400 spectrometer that was operated at a resonance frequency of 400.49 MHz for  $^1\text{H}$  and 100.70 MHz for  $^{13}\text{C}$ . Typical radiofrequency (rf) pulse lengths were 5  $\mu\text{s}$  for  $^{13}\text{C}$  and 4  $\mu\text{s}$  for  $^1\text{H}$ . A CP contact time of 0.5 ms was used. The  $^{13}\text{C}$  chemical shift was referenced externally to the  $\alpha$ -glycine C' signal at 176.49 ppm on the tetramethylsilane (TMS) scale.

A 2D  $J$ -coupling-mediated correlation experiment, CTUC–COSY, developed by Mueller and co-workers,<sup>[18]</sup> was carried out to obtain  $^{13}\text{C}$  resonance assignment. The experiment was conducted at 298 K under 9000 kHz MAS for all samples. The initial  $^{13}\text{C}$  magnetization was prepared either with  $^{13}\text{C}$  direct polarization by using a  $^{13}\text{C}$  90° pulse, or with cross polarization from  $^1\text{H}$ . The constant-time evolution period includes both the polarization transfer and  $T_1$  evolution. A soft  $^{13}\text{C}$   $\pi$  pulse of 388.9  $\mu\text{s}$  was applied on resonance with  $^{13}\text{CO}$  to selectively invert the CO signal, while a  $\pi$  pulse of 166.7  $\mu\text{s}$  was applied at 38 ppm, in the aliphatic region. The net result was that only the aliphatic  $\text{C}\alpha\text{--CX}$  ( $X = \beta, \gamma, \delta$ , etc.) cross peaks were detected in the 2D spectra. The  $T_1$  evolution times ranged from 8.8 to 11.2 ms, and the 2D spectra were processed with linear prediction in the  $\omega_1$  dimension to enhance the resolution. A  $^1\text{H}$  decoupling field of 71 kHz was used during  $T_1$ , while a weaker decoupling strength of 62 kHz was used during the  $z$  filter and the  $T_2$  acquisition time. Each 2D experiment took 18 to 24 h.

A variant of the 2D dipolar chemical-shift correlation experiment (doubled DIPSHIFT) was used to measure residue specific  $\text{C}\alpha\text{--H}\alpha$  dipolar couplings.<sup>[20,28]</sup> The dipolar doubling was achieved by using a moving  $^{13}\text{C}$  180° pulse during the rotor period while keeping  $^1\text{H}$  homonuclear decoupling on for the entire rotor period.<sup>[20]</sup> This allowed dipolar couplings to be measured with higher accuracy than the undoubled DIPSHIFT experiment. The reduction of the measured  $\text{C}\alpha\text{--H}\alpha$  dipolar coupling from the rigid-limit value was indicative of peptide backbone motion. We used MREV-8 for  $^1\text{H}$  homonuclear decoupling,<sup>[29,30]</sup> in which the  $^1\text{H}$  pulse length was 4.7  $\mu\text{s}$ . The sample was spun at 3.546 kHz. The dipolar dephasing curves were fit by using a home-written simulation program to obtain the couplings. These were divided by the MREV-8 scaling factor of 0.47 and the doubling factor of 2 to give the true coupling of each site. The true coupling was then scaled by the rigid-limit C–H dipolar coupling of 22.7 kHz to give the order parameter,  $S_{\text{CH}}$ .

The 2D  $^{13}\text{C}$ -detected  $^1\text{H}$  spin diffusion experiments were carried out with Ala-PG1 at 298 K at 5 kHz MAS. A  $^1\text{H}$   $T_2$  filter of 1 ms was used before the evolution period to remove the peptide  $^1\text{H}$  polarization. After  $^1\text{H}$  chemical-shift evolution without homonuclear decoupling, a mixing time of 25–841 ms was applied to allow  $^1\text{H}$  spin diffusion from the mobile lipids and water to the rigid peptide. The result of

the polarization transfer was detected through the peptide  $^{13}\text{C}$  signals. To obtain  $^1\text{H}$  buildup curves, the  $\text{H}_2\text{O}$  and  $\text{CH}_2$  peak heights from the 1D  $^1\text{H}$  cross sections were plotted as a function of the square root of the mixing time. The intensities were corrected for  $^1\text{H}$   $T_1$  relaxation and scaled relative to the  $\text{H}_2\text{O}$  intensity in the 100 ms spectrum. For the  $\text{CH}_2$  buildup curve, additional scaling with the fraction of the equilibrium intensity of the  $\text{CH}_2$  peak relative to the  $\text{H}_2\text{O}$  peak in the direct-polarization  $^1\text{H}$  spectrum was applied.

## Abbreviations

PG-1: protegrin-1; AMP: antimicrobial peptide; POPC: 1-palmitoyl-2-oleoyl-*sn*-glycerol-3-phosphatidylcholine; POPG: 1-palmitoyl-2-oleoyl-*sn*-glycerol-3-phosphatidylglycerol; POPE: 1-palmitoyl-2-oleoyl-*sn*-glycerol-3-phosphatidylethanolamine; CTUC–COSY: constant-time uniform-cross-peak correlation spectroscopy; DP: direct polarization; CP: cross polarization; MAS: magic-angle spinning; DIPSHIFT: 2D dipolar–chemical shift correlation.

## Acknowledgements

This work is supported by the National Institutes of Health grants GM-066976 to M.H. and AI-37945 to A.J.W. We thank Prof. Leonard Mueller for sharing the pulse sequence for the CTUC–COSY experiment and for helpful discussions in implementing the pulse sequence.

**Keywords:** antimicrobial peptides • dynamics • membranes • NMR spectroscopy • protein structure

- [1] L. Bellm, R. I. Lehrer, T. Ganz, *Expert Opin. Invest. Drugs* **2000**, *9*, 1731–1742.
- [2] J. Chen, T. J. Falla, H. Liu, M. A. Hurst, C. A. Fujii, D. A. Mosca, J. R. Embree, D. J. Loury, P. A. Radel, C. C. Chang, L. Gu, J. C. Fiddes, *Biopolymers* **2000**, *55*, 88–98.
- [3] V. N. Kokryakov, S. S. Harwig, E. A. Panyutich, A. A. Shevchenko, G. M. Aleshina, O. V. Shamova, H. A. Korneva, R. I. Lehrer, *FEBS Lett.* **1993**, *327*, 231–236.
- [4] H. Tamamura, T. Murakami, S. Horiuchi, K. Sugihara, A. Otaka, W. Takada, T. Ibuka, M. Waki, N. Yamamoto, N. Fujii, *Chem. Pharm. Bull.* **1995**, *43*, 853–858.
- [5] S. S. Harwig, A. Waring, H. J. Yang, Y. Cho, L. Tan, R. I. Lehrer, *Eur. J. Biochem.* **1996**, *240*, 352–357.
- [6] J. R. Lai, B. R. Huck, B. Weisblum, S. H. Gellman, *Biochemistry* **2002**, *41*, 12835–12842.
- [7] N. Ostberg, Y. Kaznessis, *Peptides* **2005**, *26*, 197–206.
- [8] J. J. Buffry, T. Hong, S. Yamaguchi, A. J. Waring, R. I. Lehrer, M. Hong, *Biophys. J.* **2003**, *85*, 2363–2373.
- [9] J. J. Buffry, A. J. Waring, M. Hong, *J. Am. Chem. Soc.* **2005**, *127*, 4477–4483.
- [10] J. J. Buffry, A. J. Waring, R. I. Lehrer, M. Hong, *Biochemistry* **2003**, *42*, 13725–13734.
- [11] R. Mani, J. J. Buffry, A. J. Waring, R. I. Lehrer, M. Hong, *Biochemistry* **2004**, *43*, 13839–13848.
- [12] R. Mani, M. Tang, X. Wu, J. J. Buffry, A. J. Waring, M. A. Sherman, M. Hong, *Biochemistry* **2006**, *45*, 8341–8349.
- [13] S. Yamaguchi, T. Hong, A. Waring, R. I. Lehrer, M. Hong, *Biochemistry* **2002**, *41*, 9852–9862.
- [14] R. Mani, A. J. Waring, R. I. Lehrer, M. Hong, *Biochim. Biophys. Acta Biomembr.* **2005**, *1716*, 11–18.
- [15] D. S. Wishart, B. D. Sykes, F. M. Richards, *J. Mol. Biol.* **1991**, *222*, 311–333.
- [16] M. Hohwy, C. M. Rienstra, C. P. Jaroniec, R. G. Griffin, *J. Chem. Phys.* **1999**, *110*, 7983–7992.

- [17] L. J. Mueller, D. W. Elliott, G. M. Leskowitz, J. Struppe, R. A. Olsen, K. C. Kim, C. A. Reed, *J. Magn. Reson.* **2004**, *168*, 327–335.
- [18] L. L. Chen, R. A. Olsen, D. W. Elliott, J. M. Boettcher, D. H. H. Zhou, C. M. Rienstra, L. J. Mueller, *J. Am. Chem. Soc.* **2006**, *128*, 9992–9993.
- [19] H. Zhang, S. Neal, D. S. Wishart, *J. Biomol. NMR* **2003**, *25*, 173–195.
- [20] M. Hong, J. D. Gross, C. M. Rienstra, R. G. Griffin, K. K. Kumashiro, K. Schmidt-Rohr, *J. Magn. Reson.* **1997**, *129*, 85–92.
- [21] D. Huster, X. L. Yao, M. Hong, *J. Am. Chem. Soc.* **2002**, *124*, 874–883.
- [22] R. Mani, S. D. Cady, M. Tang, A. J. Waring, R. I. Lehrert, M. Hong, *Proc. Natl. Acad. Sci. USA* **2006**, *103*, 16242–16247.
- [23] A. B. Siemer, A. A. Arnold, C. Ritter, T. Westfeld, M. Ernst, R. Riek, B. H. Meier, *J. Am. Chem. Soc.* **2006**, *128*, 13224–13228.
- [24] H. Heise, W. Hoyer, S. Becker, O. C. Andronesi, D. Riedel, M. Baldus, *Proc. Natl. Acad. Sci. USA* **2005**, *102*, 15871–15876.
- [25] S. A. Muhle, J. P. Tam, *Biochemistry* **2001**, *40*, 5777–5785.
- [26] A. Laederach, A. H. Andreotti, D. B. Fulton, *Biochemistry* **2002**, *41*, 12359–12368.
- [27] A. G. Rao, *Arch. Biochem. Biophys.* **1999**, *361*, 127–134.
- [28] M. Munowitz, W. P. Aue, R. G. Griffin, *J. Chem. Phys.* **1982**, *77*, 1686–1689.
- [29] P. Mansfield, *J. Phys. C Solid State Phys.* **1971**, *4*, 1444.
- [30] W.-K. Rhim, D. D. Elleman, R. W. Vaughan, *J. Chem. Phys.* **1973**, *59*, 3740–3749.

---

Received: June 13, 2007

Published online on September 17, 2007